Polym. Bull. (2015) 72:1497–1513
DOI 10.1007/s00289-015-1351-2

ORIGINAL PAPER

Preparation and characterization of chitosan–hydroxyapatite–glycopolymer/Cloisite 30 B nanocomposite for biomedical applications

Amal Amin[1] · Heba Kandil[1] · Hanem M. Awad[2] · Mohamed Nader Ismail[1]

Received: 24 September 2014 / Revised: 13 January 2015 / Accepted: 3 March 2015 /
Published online: 18 March 2015

Abstract A new composite was synthesized from chitosan/hydroxyapatite and glycopolymer grafted onto a Cloisite 30B clay surface (CS/HAP/clay-Gh) in aqueous media via a solvent casting and evaporation method. Another composite containing chitosan/hydroxyapatite and pristine Cloisite 30B (CS/HAP/clay) was prepared and compared with the (CS/HAP/clay-Gh). The resulting composites were characterized using various analytical tools such as Fourier transform infrared spectroscopy (FTIR), X-ray diffraction (XRD), thermal gravimetric analyses (TGA) and scanning electron microscopy (SEM). Water uptake capability or swelling was tested for each composite. The cytotoxicity of the resulting tri-component composites was tested against a breast carcinoma cell line (MCF-7), liver carcinoma cell line (HepG-2) and a normal human skin fibroblast cell line (BJ-1) by MTT [3-(4, 5-dimethyl-2-thiazolyl)-2, 5-diphenyl-2H-tetrazolium bromide] as well as LDH (lactate dehydrogenase) assay. The obtained preliminary results showed good properties for CS/HAP/clay-Gh on the way to be used in the future in the biomedical applications.

Keywords Nanocomposites · Glycopolymers · Chitosan · Hydroxyapatite · Biomedical applications

✉ Amal Amin
aamin_07@yahoo.com

[1] Polymers and Pigments Department, National Research Centre, Dokki, Giza, Egypt

[2] Department of Tanning Materials and Leather Technology, National Research Centre, Dokki, Giza, Egypt

Introduction

Tissue engineering could be an alternative strategy to renew the damaged human organs and improve the quality of life of the patient where it has been used to develop scaffolds to regenerate various tissues such as skin, liver, nerve, bone and blood vessels. [1] The success of tissue-engineered products mainly depends upon the development of degradable extracellular matrix analogs that provide a temporal support for cell adhesion, proliferation, maturation and differentiation. Natural polymers such as collagen, chitosan, fibronectin, gelatin and synthetic polymers such as polyesters and polypeptides have been used to improve the hepatocyte cell functionality where porous scaffolds with high inter-pore connectivity are desirable for the culture of hepatocytes [2, 3].

Accordingly, great attention has been paid recently to the biomimetic approaches to obtain bioinorganic and organic composite materials [4]. Natural bone is a complex of inorganic–organic nanocomposite materials, in which hydroxyapatite [HAP, $Ca_{10}(PO_4)_6(OH)_2$] nanocrystallites are well organized within self-assembled collagen fibrils [5] where the inorganic phase and a polymer phase are essentially insoluble in each other [6]. There have been many attempts to prepare bone-like biocomposites of HAP with several bioactive organic polymeric components such as collagen, chondroitin sulfate, chitosan, starch, chitin, amphiphilic peptide [7–9], poly(lactic acid) [10, 11] and polyamides [12, 13]. Chitosan (CS) and hydroxyapatite (HAP) are the best bioactive materials in bone tissue engineering where HAP is the major inorganic compound in mammalian hard tissue because of the biocompatibility and osteoconductivity [14], while CS is characterized by the high biocompatibility, biodegradability, porous structure, osteoconduction and intrinsic antibacterial nature [15]. Therefore, the composite scaffolds of CS with HAP were extensively studied for bone grafting and other tissue engineering applications [16]. However, in spite of its potential use as scaffolds in bone tissue engineering, [CS/HAP] composite scaffold has rather poor rheological properties because CS undergoes extensive swelling in water which impedes the use of CS/HAP composite scaffolds in load-bearing applications [17]. Thus, various components have been combined with CS/HAP to form effective systems for tissue engineering such as collagen, gelatin, poly (methyl methacrylate), poly (L-lactide acid), polycaprolactone, carboxymethyl cellulose, carbon nanotube and montmorillonite [15, 18–24].

Significant enhancements in nanomechanical and thermal properties were exhibited in case of [CS/HAP/montmorillonite (MMT)] scaffold compared with (CS/HAP) composite scaffold [22]. That was attributed to the high surface area and large aspect ratio of MMT as filler with HAP to reinforce chitosan and enhance the mechanical properties and thermal stability of the resulting composite.

Furthermore, porous hydroxyapatite (HA) disks have been seeded with rat hepatocytes into the peritoneal cavity of Nagase Analbuminemia rats. [25] Angiogenesis and hepatocyte viability were maintained for at least 3 weeks. Human hepatoma cell line BEL-7402 was cultured and treated with HA nanoparticles at various concentrations. It was found that hydroxyapatite nanoparticles inhibited human hepatoma BEL-7402 cell growth and induced apoptosis,

which may add a new way to use HA nanoparticles for tumor treatment [26]. Different combinatorial factors like porosity, scaffold architecture, biocompatibility, biodegradability with non-toxic degradative products and controlled release profile will provide necessary signaling cues to retain liver-specific functions.

The aim of the current work was to develop some innovative materials that can be used as scaffolds for the sustained growth of cells which may be involved in the future in the regenerative medicine and tissue engineering, because they can be potentially tailored to mimic the natural extracellular matrix in terms of structure, chemical composition and mechanical properties. Accordingly, glycopolymer was used as biocompatible polymer to modify the clay surface (e.g., Cloisite 30 B) via surface-initiated atom transfer radical polymerization (SI-ATRP). Then, the effect of grafting glycopolymer onto Cloisite 30 B on the properties of the resulting composite was studied. Generally, glycopolymer is a synthetic polymer carrying carbohydrate (sugar) moieties as pendant or terminal groups with important pharmacological and biological properties mainly because of its hydrophilic nature [27, 28]. SI-ATRP has been used to prepare well-defined polymers with interesting functionalities and architectures in addition to its ability to simultaneously grow chains from multifunctional cores or surfaces such as flat wafers, particles, colloids and polymers [29]. SI-ATRP is one of the best controlled/living surface-initiated polymerization techniques because of its tolerance to several reaction conditions in addition to relative easy preparative methodologies compared to others where SI-ATRP is performed by an in situ surface-initiated polymerization from immobilized ATRP initiator onto a solid surface [30].

Materials and methods

Materials

Cloisite 30B [31] was kindly supplied from Southern Clay Products, Inc. (Gonzales, TX) with cation-exchange capacity (CEC) as 90 meq/100 g. Chitosan was provided from Aldrich with degree of deacetylation greater than 75 %. All other chemicals were provided from Sigma–Aldrich. Roswell Park Memorial Institute (RPMI) 1640 medium and Dulbecco's Modified Eagle's Medium (DMEM) were purchased from Sigma Chem. Co. (St. Louis, MO, USA). Fetal bovine serum (FBS) was purchased from Gibco, UK.

Preparative methods

Preparation of glycomonomer (G)

The glycomonomer (G) was synthesized according to the previously reported method [32] via esterification reaction of 1, 2: 5, 6-di-*O*-isopropylidene-α-D-glucofuranose (38.4 mmol, 10 g) with methacrylic anhydride (67.1 mmol, 10 ml) in the presence of absolute pyridine (50 ml) at room temperature.

Grafting of glycopolymer (G) onto Cloisite 30 B clay surface via SI-ATRP

The nanocomposite was prepared according to the reported method by Amin et al. [33] where the ATRP surface initiator (clay–Br) was firstly prepared by treating Cloisite 30B with 2-bromoisobutyryl bromide (BIBB, 150 mmol) in the presence of triethylamine (Et_3N) and anhydrous THF. Afterward, the prepared glycomonomer was involved in controlled polymerization via SI-ATRP using clay–Br where the polymerization was carried using glycomonomer (G, 4 g, 4.9×10^{-2} mol), Clay–Br (0.2 g), 2, 2′-bpy (0.0389 g, 9.8×10^{-4} mol) and Cu (I) Br (0.0179 g, 4.9×10^{-4} mol) in xylene at 90 °C.

After certain time interval, the grafted G/clay (clay-G) nanocomposite was separated from the reaction and hydrolyzed using formic acid (80 %) to regain the hydroxyl groups in sugar rings in the grafted clay-G [34] where the OH-ended polymer (clay-Gh) nanocomposite was obtained and characterized by FTIR, XRD, TGA and SEM.

Preparation of hydroxyapatite (HAP) [35]

HAP was prepared according to the wet precipitation method reported by Katti et al. [35] by adding a liter of $CaCl_2$ solution (19.9 mol) dropwise to a liter of Na_2HPO_4 solution (11.9 mol) with continuous stirring. The solution was adjusted to 7.4 pH using 1 N NaOH. The resulting solution was kept undisturbed for 24 h, then, HAP precipitate was separated by centrifugation. The obtained precipitate was dried in vacuum oven at 50 °C for 48 h. The produced HAP was characterized by FTIR, XRD, TGA and SEM.

Synthesis of chitosan/hydroxyapatite composite (CS/HAP)

0.5 g (50 wt%) of chitosan was dissolved in 38 ml of 1 % acetic acid solution. 0.5 g (50 wt%) of HAP was dispersed in 10 ml of DI water. The HAP solution was added dropwise to the chitosan solution, and the resulting suspension was continuously stirred overnight to obtain a good dispersion of HAP in chitosan. Then, this solution was poured into a Petri dish and dried in an oven at 80 °C for 48 h to form thin sheet of CS/HAP.

Synthesis of chitosan/hydroxyapatite/clay composite (CS/HAP/clay) [22]

Firstly, 0.5 g (50 %) from chitosan was dissolved in 38 ml of 1 % acetic acid solution. Then, a suspension from 0.1 g (10 %) of clay in 15 ml H_2O was added to the chitosan solution followed by adding 0.4 g (40 %) of HAP precipitate. The resulting suspension was stirred overnight to obtain a good dispersion of HAP in chitosan. Then, it was poured into a Petri dish and dried in an oven at 80 °C for 48 h to form thin sheet of CS/HAP/clay.

Synthesis of chitosan/hydroxyapatite/clay-Gh composite (CS/HAP/clay-Gh) [22]

The same procedure described above in case of (CS/HAP/clay) was followed here but instead of using pristine Cloisite (clay), the glycopolymer grafted onto Cloisite (clay-Gh) was used.

Preparation of pure chitosan sheet (CS)

It was prepared by the same way but without adding filler to compare its properties with that of the resulting composites. CS was characterized using FTIR, XRD, TGA and SEM.

Instrumentation

Infrared measurements were carried out on Jascow FTIR-430 series infrared spectrophotometer equipped with KBr discs. Thermal gravimetric analyses (TGA) were performed on TA Instruments Q600 SDT system with heating rate 10 °C/min under nitrogen flow. X-ray diffraction (XRD) patterns were obtained via Siemens D5000 diffractometer equipped with an intrinsic germanium detector system. Scanning electron microscopy (SEM) images were collected using JSM 5410, JEOL, Japan.

Water uptake or swelling of the developed composites was performed according to a former report [15] by determining the initial weights (W_{dry}) of the previously prepared sheets (CS, CS/HAP, CS/HAP/clay and CS/HAP/clay-Gh), then by immersing them in distilled water for 24 h. Afterward, the sheets were gently removed from the beaker, dried with a filter paper to remove the excess water from the surface, and immediately weighed (W_{wet}). The water uptake (expressed as a percentage) was calculated using the following equation:

$$\text{Water uptake } (\%) = W_{wet} - W_{dry}/W_{dry} \times 100,$$

where, W_{wet} and W_{dry} = the weights of wet and dry composites, respectively.

Cell culture

Breast carcinoma cell lines (MCF-7) and liver carcinoma cell lines (HepG-2) were purchased from the American Type Culture Collection (Rockville, MD) and were maintained in RPMI-1640 medium. Normal human skin fibroblast cell line (BJ-1) was kindly supplied by Applied Research Sector, VACSERA-Egypt and was maintained in DMEM medium. All media were supplemented with 10 % heat-inactivated FBS, 100U/ml penicillin and 100U/ml streptomycin. The cells were grown at 37 °C in a humidified atmosphere of 5 % CO_2. All experiments were conducted in triplicate ($n = 3$).

In vitro cytotoxicity activities

MTT cytotoxicity assay

The cytotoxicity activity against MCF-7, HepG2 and BJ-1 human cell lines was estimated using the 3-(4,5-dimethyl-2-thiazolyl)-2,5-diphenyl-2H-tetrazolium bromide (MTT) assay, which is based on the cleavage of the tetrazolium salt by mitochondrial dehydrogenases in viable cells [36]. Cells were dispensed in a 24-well sterile microplate (2×10^5 cells/well) and incubated at 37 °C with a disk of 5 mm diameter of each tested sheet or doxorubicin (positive control) for 48 h in a serum-free medium prior to the MTT assay. After incubation, media and disks were carefully removed, 40 µl of MTT (5 mg/ml) were added to each well and then incubated for an additional 4 h. The purple formazan dye crystals were solubilized by the addition of 200 µl of acidified isopropanol. The absorbance was measured at 570 nm using a microplate ELISA reader (Biorad, USA). The relative cell viability was expressed as the mean percentage of viable cells compared to the untreated controlled cells [37].

Lactate dehydrogenase (LDH) assay

To determine the effect of each sheet on the membrane permeability in MCF-7, HepG2 and BJ-1 cell lines, a lactate dehydrogenase (LDH) release assay was used [36]. The cells were seeded in 24-well culture plates at a density of 2×10^5 cells/well in 500 µl volume and were allowed to grow for 18 h before treatment. After treatment with a disk of 5 mm diameter of each tested sheet or doxorubicin (positive control), the plates were incubated for 48 h, then, the disks were removed. The supernatant (40 µl) was transferred to new 96-well sterile microplate to determine LDH release and 6 % triton X-100 (40 µl) was added to the original plate for determining the total LDH. An aliquot of 0.1 M potassium phosphate buffer (100 µl, pH 7.5) containing 4.6 mM pyruvic acid was mixed to the supernatant using repeated pipetting. Then, 0.1 M potassium phosphate buffer (100 µl, pH 7.5) containing 0.4 mg/ml reduced β-NADH was added to the wells. The kinetic changes were determined for 1 min using ELISA microplate reader at wavelength 340 nm. This procedure was repeated with 40 µl of the total cell lysate to determine total LDH. The percentage of LDH release was determined by dividing the LDH released into the media by the total LDH following cell lysate in the same well [37].

Results and discussions

Chitosan/hydroxyapatite/glycopolymer grafted-clay (e.g., Cloisite) nanocomposite (CS/HAP/clay-Gh) has been prepared upon several steps according to Scheme 1 where Cloisite 30B surface was firstly converted to ATRP surface initiator (clay–Br) by treating it with ATRP initiator (2-bromoisobutyryl bromide). Glycomonomer (G) was prepared and characterized as mentioned in the literature [32]. Then, G was polymerized via SI-ATRP using clay–Br as surface initiator to form clay-G which

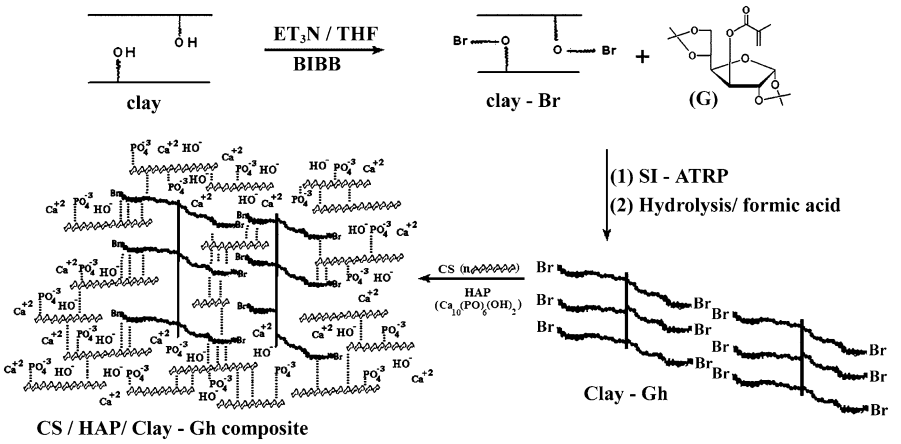

Scheme 1 Snthesis of CS/HAP/clay-Gh composite

was separated and purified from copper residues of ATRP. The clay-G was subjected to hydrolysis reaction using formic acid where OH-ended polymer clay nanocomposite (clay-Gh) evolved. The aim of the last step was to regain the hydroxyl groups in clay-G for complete beneficial use of the resulting (clay-Gh) nanocomposite. The resulting clay-Gh was then used in preparing the CS/HAP/Clay-Gh composite. Afterward, three composites were prepared, one of them was CS/HAP composite and the others were CS/HAP/clay and CS/HAP/clay-Gh composites. The properties of the prepared composites were studied, especially the composites containing glucose units, to identify the influence of its presence inside the composites.

Thermal stability of the prepared composites

TGA was performed for CS, CS/HAP, CS/HAP/clay and CS/HAP/clay-Gh as shown in (Fig. 1) to reveal the thermal stability of the prepared composites. From the TGA curves, it was observed that the onset points for the degradation of the prepared composites were variable, i.e., the onset point for CS sheet was at 250 °C, while for CS/HAP, it increased to 265 °C. The onset point increased to 270 and 272 °C for CS/HAP/clay and CS/HAP/clay-Gh, respectively. The slight temperature differences observed for the CS/HAP/clay and CS/HAP/clay-Gh composites might be due to the presence of some covalent interactions occurred as in case of CS/HAP/clay-Gh between clay-Gh and chitosan. The weight loss below 300 °C was attributed to the water evaporation and the loss of chitosan moieties.

At high temperatures as 500 °C, chitosan sheet lost all its weight, whereas no weight loss was observed in case of CS/HAP, CS/HAP/clay and CS/HAP/clay-Gh composites and that was ascribed to the presence of HAP which increased the thermal stability of the composites. However, it was observed that the thermal stability of CS/HAP/clay and CS/HAP/clay-Gh was slightly higher than that of

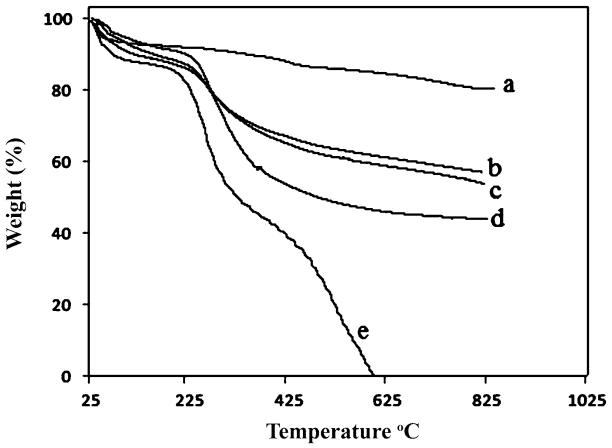

Fig. 1 TGA of (HAP) (*a*), CS/HAP/clay-Gh (*b*), CS/HAP/clay (*c*), CS/HAP (*d*) and CS film (*e*)

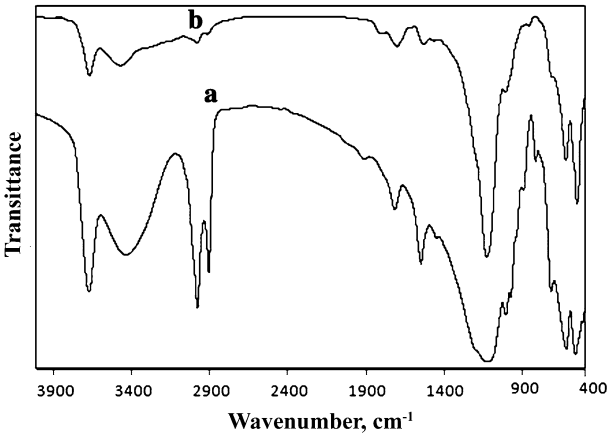

Fig. 2 FTIR of clay (*a*) and clay-Gh (*b*)

CS/HAP and this was attributed to, beside the presence of HAP, the existence of clay platelets which played an important role in providing a thermal barrier and delaying the weight loss of chitosan. The previous data indicated that the prepared composites were highly stable at higher temperatures.

Chemical structures of the resulting composites

The chemical structures of HAP, clay, clay-Gh, CS film, CS/HAP, CS/HAP/clay and CS/HAP/clay-Gh composites were identified by FT-IR analyses in the region of 4000–400 cm^{-1} as shown in Figs. 2, 3. For HAP, the spectrum showed the characteristic absorption bands of synthetic HAP at 1636, 1032, 962 and at

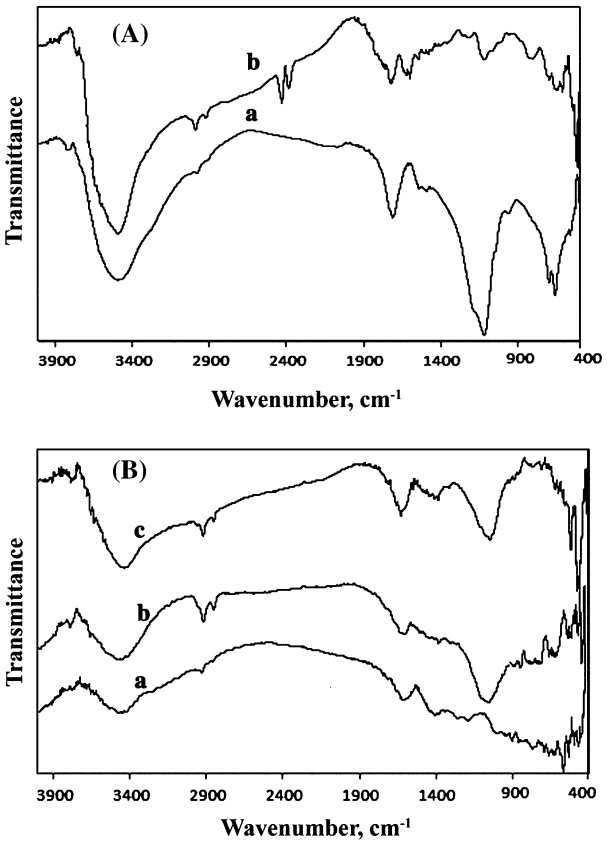

Fig. 3 FTIR of **A** HAP (*a*) and CS film (*b*), **B** CS/HAP (*a*), CS/HAP/clay (*b*) and CS/HAP/clay-Gh (*c*)

564 cm^{-1} for phosphate group $(PO_4)^{-3}$ while the peaks of $(CO_3)^{-2}$ appeared at 1464–1408 cm^{-1} and at 874 cm^{-1} but the hydroxyl group (O–H) appeared at 3447 cm^{-1}. The FTIR spectrum of CS film (Fig. 3A) showed the typical characteristic absorption bands of chitosan where carbonyl group (C=O) appeared at 1734 cm^{-1}, but C–H stretching and bending appeared at 1414 and 1379 cm^{-1}, respectively. Amine stretching frequency (N–H) and pyranose (C–O–C) stretching mode appeared at 1145, 1077 and 1022 cm^{-1}, respectively. Moreover, the characteristic stretching frequency of clay (Si–O–Si) was observed at 1100 cm^{-1} and OH stretching frequency appeared at 3500 cm^{-1}. All these characteristic peaks appeared in FTIR spectra of the prepared composites (Fig. 3B), However, in the spectrum of CS/HAP/clay-Gh composite, it was noticed that the peak at 3500 cm^{-1} was very broad which was attributed to the presence of the hydroxyl groups in clay-Gh which played an important role in forming hydrogen bonds between the components of the composite.

X-ray diffraction studies

The XRD plots of clay, clay-Gh, CS film, HAP, CS/HAP, CS/HAP/clay and CS/HAP/clay-Gh were recorded as shown in Figs. 4 and 5. A distinct peak appeared in case of clay (Fig. 4) at ($2\theta = 6.896$; $d = 18.2$ A°) where after grafting the glycopolymer, that peak disappeared which indicated that exfoliated structure was obtained. XRD plots of HAP and CS films showed as in Fig. 4, the characteristic peaks for both of HAP and CS where for CS film, its' corresponding main peaks were observed at $2\theta = 20$ (maximum intensity) and 22.5, while the major corresponding peaks of HAP appeared at $2\theta = 26.3$, 30.1, 31.6, 32.3, 45.3 and 49.2. In all XRD spectra of the three composites (i.e., CS/HAP, CS/HAP/clay and CS/HAP/clay-Gh; Fig. 5), there were three observed diffraction peaks at $2\theta = 20.0$, 26.3 and 32.3 which revealed the presence of both CS and HAP in the prepared composites. In case of XRD spectra of CS/HAP/clay-Gh, it was observed that the distinct peak of clay at $2\theta = 6.8$ disappeared here which indicated that the clay was well dispersed in chitosan matrix and exfoliated structure was obtained.

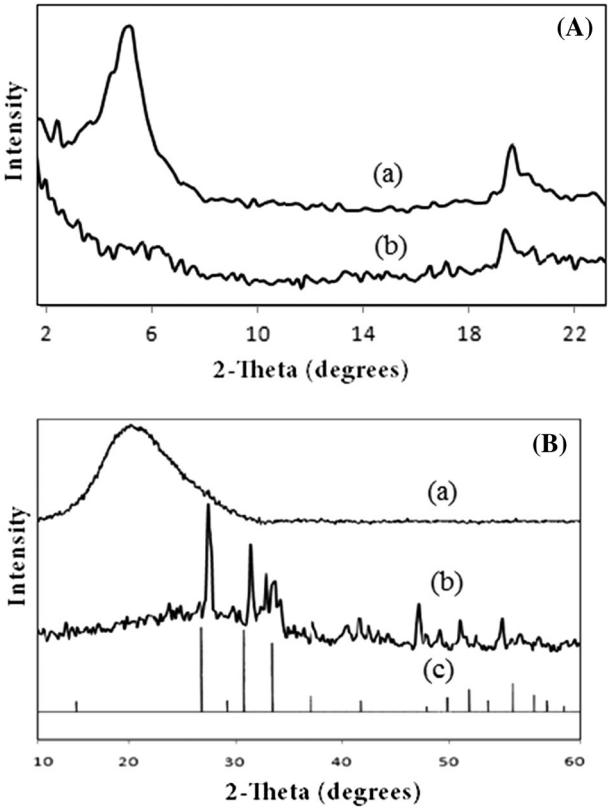

Fig. 4 XRD of **A** clay and clay-Gh (*b*). **B** CS (*a*) and HAP (*b*, *c*)

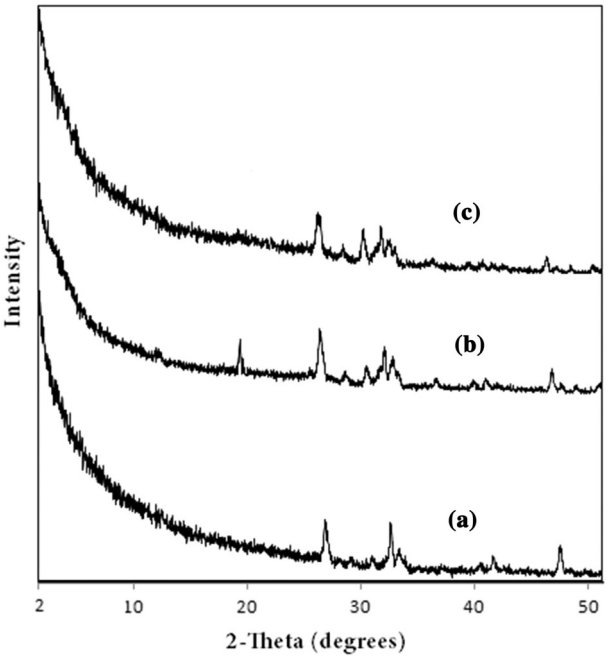

Fig. 5 XRD of CS/HAP (*a*), CS/HAP/clay (*b*) and CS/HAP/Clay-Gh (*c*)

Morphology studies of the composites

The SEM images were illustrated as shown in Fig. 6 for low and high magnification pictures of CS, HAP, clay-Gh, CS/HAP, CS/HAP/clay and CS/HAP/clay-Gh. Generally, in each case, the darker part represented the polymer, and the lighter part was assigned to the fillers. According to the SEM images, HAP particles were uniformly dispersed in the chitosan (Fig. 6). Uniform distribution of HAP particles and clay in the polymer matrix was observed which might be due to the electrically charged nature of chitosan network.

Water uptake

The goal of preparing CS/HAP, CS/HAP/clay and CS/HAP/clay-Gh composites was to apply them in the biomedical applications such as bone tissue engineering and other bone repairing applications; so, the water uptake capability was tested for each composite. It was evident from the results that adding HAP and clay either treated or untreated to pure chitosan led to a significant decrease in the degree of water absorption of chitosan. However, it was observed that the water uptake in case of CS/HAP/clay-Gh was less than that in case of CS/HAP and CS/HAP/clay (Fig. 7).

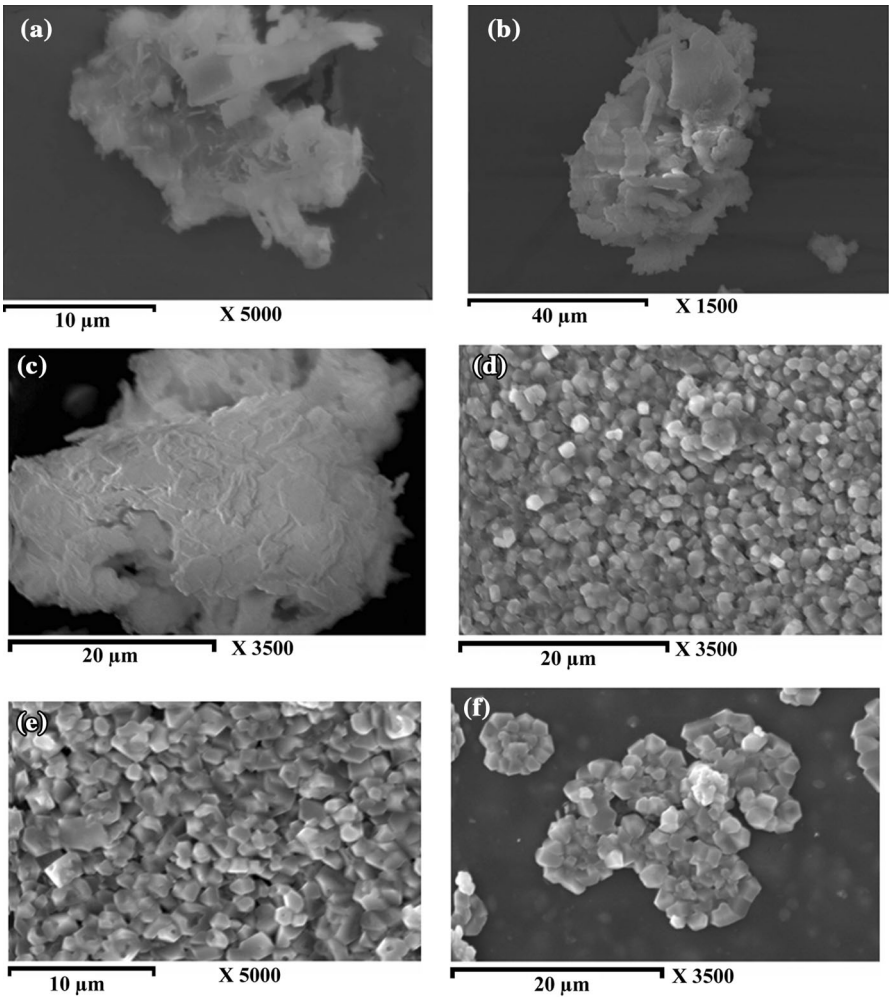

Fig. 6 SEM of CS film (**a**), HAP (**b**), clay-Gh (**c**), CS/HAP (**d**), CS/HAP/clay (**e**) and CS/HAP/clay-Gh (**f**)

In vitro cytotoxicity activity

In this study, CS/HAP, CS/HAP/clay and CS/HAP/clay-Gh were examined in vitro for their cytotoxicity activities against MCF-7, HepG2 and BJ-1 cell lines using MTT assay, this assay aimed at measuring the percentage of the intact cells compared to the control, as well as LDH assay to measure the cellular membrane permeabilization (rupture) and severe irreversible cell damage (Table 1). The results for the three sheets did not show any significant cytotoxicity, after 48 h, in all the three tested cell lines as they all showed very weak cytotoxicity activity ranged from 5.2 to 17.5 %. CS/HAP/clay-Gh sheet showed the least toxic effect on all cell

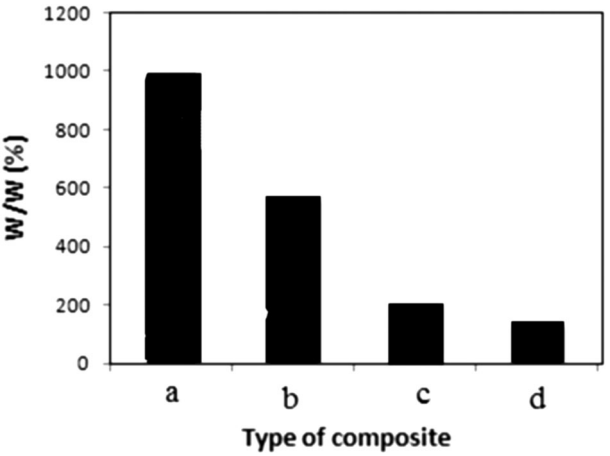

Fig. 7 Water uptake of CS film (*a*), CS/HAP (*b*), CA/HAP/clay (*c*) and CS/HAP/clay-Gh (*d*)

Table 1 Measuring cytotoxicity of the prepared composites against MCF-7, HepG2 and BJ-1 cell lines using MTT, LDH assay

Sheet (0.5 cm diameter)	% Growth inhibition (% of control)					
	MCF-7		HepG2		BJ-1	
	MTT	LDH	MTT	LDH	MTT	LDH
CS/HAP	15.9 ± 2.1	16.5 ± 1.9	12.4 ± 3.8	13.8 ± 1.9	13.5 ± 2.4	14.8 ± 2.7
CS/HAP/clay	17.5 ± 1.7	15.8 ± 2.5	17.2 ± 1.4	17.8 ± .9	15.3 ± 2.8	14.3 ± 2.5
CS/HAP/clay-Gh	10.1 ± 1.5	9.2 ± 3.2	9.1 ± 2.7	10.2 ± 2.1	5.2 ± 1.5	6.2 ± 1.9

lines. By visualized analysis of the cells under microscopy, it was observed that only the area under each disk of these three sheets did not show any viable cells and this was explained by the fact that each disk of these sheets covered the area under it and therefore it prevented the media and the humidity as well as the CO_2 to reach this area which resulted in the death of the cells only in these covered areas without any toxic effect on the other cells. These results were in agreement with the previously reported data which indicated that similar composite nanoparticles containing HAP did not show significant toxicity where in one study, the in vitro biocompatibility and the proliferation of bone marrow stromal cells (BMSCs) were evaluated on *n*-CS/HAP composite membranes using MTT assay. Nevertheless, after 7 days, the cells cultured with the composite membrane of 40 % *n*-HAP got the best proliferation and the cells on pure CS membrane held the lowest proliferation among the three investigated membrane groups (pure CS, 40 % *n*-HAP and 60 % *n*-HAP). The results showed that n-HA and its content had obvious effect on the proliferation of BMSCs [38]. In addition, it has been reported that at 50 mg/L HAP nanoparticles, no significant cytotoxicity was observed on MCF-7. However, at higher concentrations, nano-HAP inhibited the proliferation of MCF-7 cells in a

dose-dependent manner. Induction of apoptosis might be accounted for the anti-proliferation effect [39].

In addition, the biological response of pre-osteoblasts (MC3T3-E1) on the nanocomposite scaffolds of medium-MW chitosan scaffolds with 0.5, 1 and 2 % *n*-HAP was found to be superior in terms of improved cell attachment, higher proliferation, and well-spread morphology with respect to chitosan scaffold. In the composite scaffolds, cell proliferation was about 1.5 times greater than pure chitosan after 7 days of culture and beyond, as implied by qualitative analysis via fluorescence microscopy and quantitative study through MTT assay. The observations related to well-developed structure morphology, physicochemical properties and superior cytocompatibility suggested that chitosan–*n*-HAP porous scaffolds are potential candidate materials for bone regeneration although it is necessary to enhance the mechanical properties of the nanocomposite [40].

Furthermore, in another study, composite films were prepared from chitosan (CS) and gelatin (G) with the addition of HAP. The cell affinities were studied using human osteosarcoma (SaOs-2) cell line. The cell proliferation and spreading of Saos-2 cells were found to be higher for the films with high gelatin content and no HAP; whereas for HAP-containing composites, higher cell affinities were obtained for the samples which had high chitosan content (CS:HAP = 66.7:33.3 %) where for 7 days, no toxicity and good proliferation were observed [41].

Finally, it has been reported that, greater cell viability and cell proliferation were measured on MC3T3-E1 cell lines (osteoblast) treated with three kinds of HAP nanoparticles (neutral, positive, and untreated), among which positively charged HAP nanoparticles showed the strongest improvement for cell viability and cell proliferation even after 7 days [42].

Conclusion

The rapidly developing tissue engineering field requires novel processing methods and designs of scaffolds and membranes for guided tissue regeneration. Embedding of HAP into polymeric matrices containing CS has gained much attraction since HAP-type crystals form the main inorganic component of the bone structure and can be used as supporting materials for tissue engineering. Therefore, CS/HAP/clay composite has been recommended for bone regeneration and for other different applications related to tissue engineering to regenerate various tissues of skin, liver, nerve, bone and blood vessels by developing the suitable scaffolds for that.

Accordingly, CS/HAP/clay-Gh composite was prepared through solvent casting and evaporation methods. FTIR, XRD, TGA, SEM, swelling measurements and cytotoxicity test were applied to investigate the effect of grafting biocompatible polymer onto clay surface on the properties of the resulting composite. The results showed that the CS/HAP/clay-Gh tri-component composite is an extremely potent class of biomaterials.

Also, the results of this study revealed that the composite containing glycopolymer-modified Cloisite (i.e., chitosan/hydroxyapatite/clay-Gh) showed improved thermal stability and no significant toxicity on all cell lines as compared to the

composite with pristine Cloisite. Therefore, this composite could be used as a suitable material for the delivery of bioactive compounds as well as tissue engineering.

In addition, the in vitro results may provide useful information for the investigations related to HAP composite nanoparticles for the applications in gene delivery and intracellular drug delivery. Such a composite membrane may provide a good prospect for further research and development in biodegradable guided bone regeneration (GBR) membrane for future applications as well.

References

1. Kuppan P, Vasanthan KS, Sundaramurthi D, Krishnan UM, Sethuraman S (2011) Development of poly(3-hydroxybutyrate-co-3-hydroxyvalerate) fibers for skin tissue engineering. Effects of topography, mechanical, and chemical stimuli. Biomacromolecules 12:3156–3165
2. Slaughter BV, Khurshid SS, Fisher OZ, Khademhosseini A, Peppas NA (2009) Hydrogels in regenerative medicine. Adv Mater 21:3307–3329
3. Wu C, Pan J, Bao Z, Yu Y (2007) Fabrication and characterization of chitosan microcarriers for hepatocyte culture. J Mater Sci Mater Med 18:2211–2214
4. Kim GM (2010) Fabrication of bio-nanocomposite nanofibers mimicking the mineralized hard tissues via electrospinning process. In: Kumar A (ed) Nanofibers. Intech, Croatia, pp 69–88
5. Swetha M, Sahithi K, Moorthi A, Srinivasan N, Ramasamy K, Selvamurugan N (2010) Biocomposites containing natural polymers and hydroxyapatite for bone tissue engineering. Int J Biol Macromol 47:1–4
6. Gasser B (2000) About composite materials and their use in bone surgery. Injury 31:D48–D53
7. Kikuchi M, Itoh S, Ichinose S, Shinomiya K, Tanaka J (2001) Self-organization mechanism in a bone-like hydroxyapatite/collagen nanocomposite synthesized in vitro and its biological reaction in vivo. Biomaterials 22:1705–1711
8. Yamaguchi I, Tokuchi K, Fukuzaki H, Koyama Y, Takakuda K, Monma H, Tanaka J (2000) Preparation and mechanical properties of chitosan/hydroxyapatite nanocomposites. Key Eng Mater 192–195:673–676
9. Chen F, Wang ZC, Lin CJ (2002) Preparation and characterization of nano-sized hydroxyapatite particles and hydroxyapatite/chitosan nanocomposite for use in biomedical materials. Mater Lett 57:658–662
10. Liao SS, Cui FZ, Zhang W, Feng QL (2004) Hierarchically biomimetic bone scaffold materials: nano-HA/collagen/PLA composite. J Biomed Mater Res Part B Appl Biomater 69B:158–165
11. Deng XM, Hao JY, Wang CS (2002) Preparation and mechanical properties of nanocomposites of poly(D, L. lactide) with Ca-deficient hydroxyapatite nanocrystals. Biomaterials 22:2867–2873
12. Wei J, Li YB, Chen WQ, Zuo Y (2003) A study on nanocomposite of hydroxyapatite and polyamide. J Mater Sci 38:3303–3306
13. Hung M, Feng JQ, Wang JX, Zhang XD, Li YB, Yan YG (2003) Synthesis and characterization of nano-HA/PA66 composites. J Mater Sci Mater Med 14:655–660
14. Pighinelli L, Kucharska M (2013) Chitosan–hydroxyapatite composites. Carbohydr Polym 93:256–262
15. Venkatesan J, Qian ZJ, Ryu B, Kumar NA, Kim SK (2011) Preparation and characterization of carbon nanotube-grafted-chitosan—natural hydroxyapatite composite for bone tissue engineering. Carbohydr Polym 83:569–577
16. Venkatesan J, Venkatesan J, Pallela R, Bhatnagar I, Kim SK (2012) Chitosan–amylopectin/hydroxyapatite and chitosan–chondroitin sulphate/hydroxyapatite composite scaffolds for bone tissue engineering. Int J Biol Macromol 51:1033–1042
17. Mututuvari TM, Harkins AL, Tran CD (2013) Facile synthesis, characterization, and antimicrobial activity of cellulose–chitosan–hydroxyapatite composite material: a potential material for bone tissue engineering. J Biomed Mater Res, Part A 101:3266–3277

18. Li J, Chen Y, Yin Y, Yao F, Yao K (2007) Modulation of nano-hydroxyapatite size via formation on chitosan–gelatin network film in situ. Biomaterials 28:781–790
19. Zhang L, Tang P, Zhang W, Xu M, Wang Y (2010) Effect of chitosan as a dispersant on collagen-hydroxyapatite composite matrices. Tissue Eng Part C Methods 16:71–79
20. Xiao X, Liu R, Huang Q, Ding X (2009) Preparation and characterization of hydroxyapatite/polycaprolactone-chitosan composites. J Mater Sci Mater Med 20:2375–2383
21. Liuyun J, Yubao L, Chengdong X (2009) A novel composite membrane of chitosan-carboxymethyl cellulose polyelectrolyte complex membrane filled with nano-hydroxyapatite I. Preparation and properties. J Mater Sci Mater Med 20:1645–1652
22. Katti KS, Katti DR, Dash R (2008) Synthesis and characterization of a novel chitosan/montmorillonite/hydroxyapatite nanocomposite for bone tissue engineering. Biomed Mater 3:034122
23. Kim S, Kim Y, Yoon T, Park S, Cho I, Kim E, Kim I, Shin J (2004) The characteristics of a hydroxyapatite–chitosan–PMMA bone cement. Biomaterials 25:5715–5723
24. Niu X, Feng Q, Wang M, Guo X, Zheng Q (2009) Porous nano-HA/collagen/PLLA scaffold containing chitosan microspheres for controlled delivery of synthetic peptide derived from BMP-2. J Control Release 134:111–117
25. Higashiyama S, Noda M, Muraoka S, Hirose M, Ohgushi H, Kawase M (2003) Transplantation of hepatocytes cultured on hydroxyapatite into Nagase analbuminemia rats. J Biosci Bioeng 96(1):83–85
26. Liu ZS, Tang SL, Ai ZL (2003) Effects of hydroxyapatite nanoparticles on proliferation and apoptosis of human hepatoma BEL-7402 cells. World J Gastroenterol 9(9):1968–1971
27. Pearson S, Chen G, Stenzel MH (2011) Synthesis of glycopolymers. In: Narain R (ed) Engineered carbohydrate-based materials for biomedical applications: polymers, surfaces, dendrimers, nanoparticles, and hydrogels. Wiley, Canada, pp 1–108
28. Li ZC, Liang YZ, Chen GQ, Li FM (2000) Synthesis of amphiphilic block copolymers with well defined glycopolymer segment by atom transfer radical polymerization. Macromol Rapid Commun 21:375–380
29. Pyun J, Kowalewski T, Matyjaszewski K (2003) Synthesis of polymer brushes using atom transfer radical polymerization. Macromol Rapid Commun 24:1043–1059
30. Yoon KR, Ramaraj B, Lee S, Yu JS, Choi IS (2009) Surface-initiated atom transfer radical polymerization of 3-O-methacryloyl-1,2:5,6-di-O-isopropylidene-α- D-glucofuranoside onto gold surface. J Biomed Mater Res A 88A:735–740
31. Datta H, Bhowmick AK, Singha NK (2008) Tailor-made hybrid nanostructure of poly(ethyl acrylate)/clay by surface-initiated atom transfer radical polymerization. J Polym Sci Part A Polym Chem 46:5014–5027
32. Ohno K, Tsujii Y, Fukuda T (1998) Synthesis of a well-defined glycopolymer by atom transfer radical polymerization. J Polym Sci Part A Polym Chem 36:2473–2481
33. Amin A, Kandil HS, El-Shafie K, Ramadan A, Ismail MN (2013) Preparation of homo and block glycopolymers/layered silicate nanocomposites by surface-initiated atom transfer radical polymerization. J Colloid Sci Biotechnol 2:226–235
34. Gao C, Muthukrishnan S, Li W, Yuan J, Xu Y, Müller AHE (2007) Linear and hyperbranched glycopolymer-functionalized carbon nanotubes: synthesis, kinetics, and characterization. Macromolecules 40:1803–1815
35. Katti KS, Turlapati P, Verma D, Bhowmik R, Gujjula PK, Katti DR (2006) Static and dynamic mechanical behavior of hydroxyapatite–polyacrylic acid composites under simulated body fluid. Am J Biochem Biotechnol 2:73–79
36. Hamdy NA, Anwar MM, Abu-Zied KM, Awad HM (2013) Synthesis, tumor inhibitory and antioxidant activity of new polyfunctionally 2-substituted 5,6,7,8-tetrahydro-naphthalene derivatives containing pyridine, thioxopyridine and pyrazolo-pyridine moieties. Acta Pol Pharm Drug Res 70:987–1001
37. Almajhdi FN, Fouad H, Khalil KA, Awad HM, Mohamed SHS, Elsarnagawy T, Albarrag AM, Al-Jassir FF, Abdo HS (2014) In-vitro anticancer and antimicrobial activities of PLGA/silver nanofiber composites prepared by electrospinning. J Mater Sci Mater Med 25:1–9
38. Cheng X, Li Y, Zuo Y, Zhang L, Li J, Wang H (2009) Properties and in vitro biological evaluation of nano-hydroxyapatite/chitosan membranes for bone guided regeneration. Mater Sci Eng C 29:29–35
39. Ramovatar M, Kavindra KK, Madhu R, Paulraj R (2012) Effects of hydroxyapatite nanoparticles on proliferation and apoptosis of human breast cancer cells (MCF-7). J Nanopart Res 14:712

40. Thein-Han WW, Misra RDK (2009) Biomimetic chitosan–nanohydroxyapatite composite scaffolds for bone tissue engineering. Acta Biomater 5:1182–1197
41. Isikli C, Hasirci N (2012) Surface and cell affinity properties of chitosan-gelatin-hydroxyapatite composite films. Key Eng Mater 493–494:337–342
42. Chen L, Mccrate JM, Lee JCM, Li H (2011) The role of surface charge on the uptake and biocompatibility of hydroxyapatite nanoparticles with osteoblast cells. Nanotechnology 22:105708